Iran J Earth Sci., 2026; 18(2): 203-220

Iranian Journal of Earth Sciences (IJES)

https://doi.org/10.57647/j.ijes.2025.16945

Research Article

Reducing Geopressure Related Non-Productive Drilling Downtime: A Case of Recent Proposed HPHT Deep Exploration Well, Onshore-Shelf, Niger Delta Basin, Nigeria

Charles Chibueze Ugbor, David Odofin, Chukwudike Gabriel Okeugo*

Department of Geology, University of Nigeria, Nsukka, Enugu State Nigeria

***Corresponding author:** chukwudike.okeugo@unn.edu.ng

Article History:

Received:
21 June 2024

Revised:
21 November 2024

Accepted:
14 December 2024

Published online:
24 June 2025

Published in Issue:
30 June 2026

Abstract

Poorly predicted abnormal pressure has contributed to drilling non-productive downtime in most exploration fields in Niger Delta Basin. However, several advances have been made to improve pressured-related non-productive downtime during drilling. Despite the advances, it has become more critical during pre-drill geopressure prediction. This study has estimated Eaton's and Bower's prediction models ahead of the drilling bit in a recent drill campaign. The aim is to reduce non-productive downtime for a proposed 1000ft untested hydrocarbon reservoir (Kulon XII deep well) in the Onshore/Shelf, Niger Delta Basin. The study projected the accuracy level of Eaton's or Bower's prediction model ahead of drilling the Kulon XII deep well. Offset well result closest to the proposed High Pressure, High Temperature (HPHT) Kulon XII deep exploration well confirmed that pore pressure prediction at shallow depths (less than 11,750ft) confirmed that Eaton's model predicted pore pressure below hydrostatic gradient, while Bowers model at same condition overestimated it. At depths greater than 12,000ft, the Eaton and Bowers prediction model matched with the measured pore pressure. Both models were used to predict pore pressure at deeper intervals of the proposed well. The predicted pore pressure profile from the offset well revealed the onset of mild overpressure at depths greater than 11,900ft. Therefore, the seismic velocity was scaled by a factor of +/- 5% to determine the mud weight that will be required for drilling of the Kulon XII deep well in order not to experience kick at depths greater than 13,000ft.

Keyword: Reducing Geopressure, Drilling downtime, High Pressure, High Temperature, Eaton Prediction, Bowers Prediction, Niger Delta Basin

Cite this article: Ugbor, C. C., Odofin, D. & Okeugo, C. G., (2026). Iranian Journal of Earth Sciences, Reducing Geopressure Related Non-Productive Drilling Downtime: A Case of Recent Proposed HPHT Deep Exploration Well, Onshore-Shelf, Niger Delta Basin, Nigeria, 18(2): 203-220. https://doi.org/10.57647/ijes.2025.16945

1. Introduction

Abnormal pore pressures, particularly overpressures, if not accurately predicted before drilling and while drilling can greatly increase drilling non-productive time (NPT) and cause serious drilling incidents such as well blowouts, pressure kicks, and fluid influx. Over the years, it is a major cause of hazard during oil and gas exploration and production in the Niger Delta Basin and other basins of the

world (York et. al., 2009; Hamid et. al., 2016; Karimiazar et al. 2023). According to Badri et. al., (2000), overpressures occur when pore pressure exceeds formation hydrostatic pressure and is related to certain environmental conditions in a given earth section. In the Niger Delta basin, overpressure is a major concern, and understanding the distribution of pore pressure in the subsurface is very essential for drilling efficient and safe wells with optimum mud weights (Badri et. al., 2000). This is because drilling into an overpressured formation with the wrong mud weight mainly results in drilling incidents such as wellbore instability (due to shear failure), loss in circulation (a result of hydraulic fracturing of the formation due to mud pressure), possible case failure and even pressure kick and blowout (Skalle and Podi, 1998; Holand and Skalle, 2001; Dehghan and Yazdi 2023). Several factors have been linked as the root causes of overpressure in the geological formation and such factors include an increase in compressive stress (caused by disequilibrium compaction and tectonic compression); fluid volume increase or expansion as a result of an increase in temperature (aqua thermal pressuring), diagenesis, hydrocarbon generation, and cracking to gas; fluid migration and buoyancy, stress and compartmentalized lithology in an aqueous environment (Osborne and Swarbrick, 1997; Swarbrick and Osborne 1998; Swarbrick, 1999 and Velázquez-Cruz et. al., 2017). According to Zijian et. al., (2015), these factors are mainly driven by mechanical mechanisms relating to the loading and unloading process. During the loading process, porosity decreases as the effective stress increases. In the same way, interval transit time reduces, and the formation density increases. The unloading process occurs after primary compaction and under-compaction have taken place in the formation. Table 1 summarizes, the relationship between the causes of overpressure, interval transit time, formation density, and mechanical mechanism (loading and unloading process). In recent times, several methods have been used to predict overpressured zones in most exploration fields including the Niger Delta Basin fields. These methods use drilling data, wireline logs, and geophysical data (Yu et. al., 2020, Zhang et. al., 2022, Das and Maiti 2024) to train a supervised or unsupervised Machine Learning Languages (MLL) algorithms. Machine Learning Language such as multiple linear regression (MLR) model, Decision Tree Regression (DTR), Adaboost (ADA), Random Forest (RF), Transparent Open Box (TOB) etc, have attained some reliable results and enhance some levels of accuracy in predicting pore pressures in many exploration projects (Das and Maiti 2024, Zhang et. al., 2022). However, during the planning and drilling stage for any deeper (HPHT) exploration well, pore pressure prediction requires more understanding of relationships between available data, geological processes and factors responsible for overpressure in the formation. This paper combined the Eatons and Bowers methods of pore pressure prediction using offset well and seismic velocity data to predict formation pore pressure for the proposed Kulon XII HPHT deep exploration well in Kulon Field. This study will serve as a guide for the prediction of geopressure in the Niger Delta Basin and to match the accuracy of the geopressure prediction models before drilling deeper well in the shelf zones of the basin to avert non-productive downtime due to abnormal or overpressures.

2. Geologic and Structural Background

The geological and structural framework of the Niger Delta basin has been related to the stresses that accompanied the separation of African and South American plates (Steve et. al., 2002). According to Lehner and De Ruiter (1977), the separation led to the opening of the South Atlantic which later was controlled by cretaceous fracture zones (trenches and ridges) in the deep Atlantic. These fracture zone ridges were subdivided into individual basins by boundary faults of the Cretaceous Benue-Abakaliki trough (Lehner and De Ruiter, 1977). Several authors stated that during the mid-Eocene, a major regression that resulted in the formation of the present-day Niger Delta started. According to Reijers (2011), the Cretaceous Abakaliki trough formed the northeastern boundary of the Niger Delta Basin towards the Abakaliki High and further East-South-East by the Calabar flank (a hinge line bordering the adjacent Precambrian). Later, gravity induces growth tectonics became the primary deformational process leading to the formation of five parallel fault-bounded depositional belts (depo-belts) that dip in the direction of sediment progradation (Short and Stauble 1967; Weber and Daukoru, 1975; Reijers, 2011). These depo-belts includes Northern Delta depobelt, Greater Ugheli depobelt, Central Swamp depobelt, Coastal Swamp depobelt, Offshore depobelt. These gravity-induced tectonics generated complex structures such as shale diapirs, roll-over anticlines, collapsed growth fault crests, back-to-back features, and steeply dipping, closely spaced flank faults (Evamy et. al., 1978; Xiao and Suppe, 1992). The stratigraphy of the Central Swamp depobelt is represented by marine shales of the Akata Formation, followed by the Agbada Formation which is made up of interbedded shallow marine and fluvial sands, silts, and clays that are typical of a paralic setting. The deposition of the Benin Formation capped the stratigraphy with massive continental alluvial sands Figs. 1 and 2.

10.57647/ijes.2025.16945

Table 1. Relationship between the causes of overpressure, a mechanical mechanism, interval transit time, formation density, and prediction model. (After Zijian et. al., 2015; Okocha et. al., 2020)

Cause of Abnormal overpressure		Mechanical mechanism	Interval transit time	Formation Density	Prediction Model
The change in Pore volume	Under compaction	Loading	Decrease	Decrease	Eaton Model
Structural Tectonic movement	Compression from in-situ stress				Bowers loading model
	Shear from in-situ stress	Unloading	Decrease	Remain Unchanged	Modified Eaton model
	Uplift of the formation				
	Aquathermal expansion				
	Clay diagenesis				
The change of Formation pore fluid volume	Hydrocarbon Generation				Bowers unloading model
	Fluids migration				
	Permeation				
	Hydraulic head				

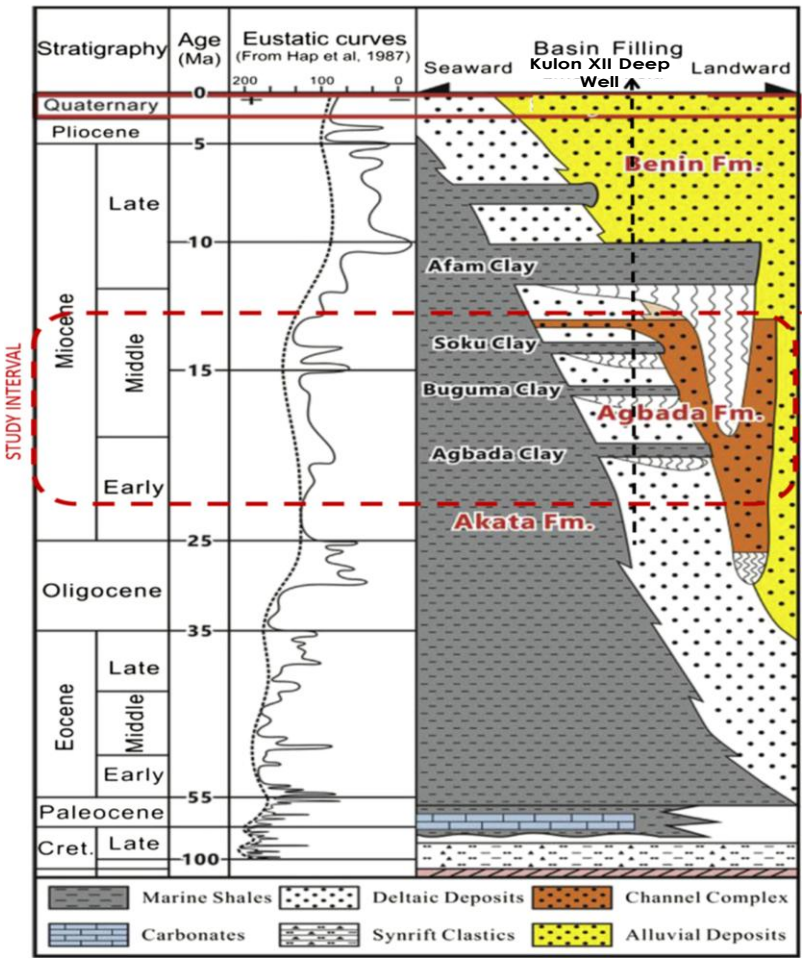

Figure 1. Niger Delta regional stratigraphy (modified after Corredor et al., 2005). **Note:** The dotted red line is the study interval

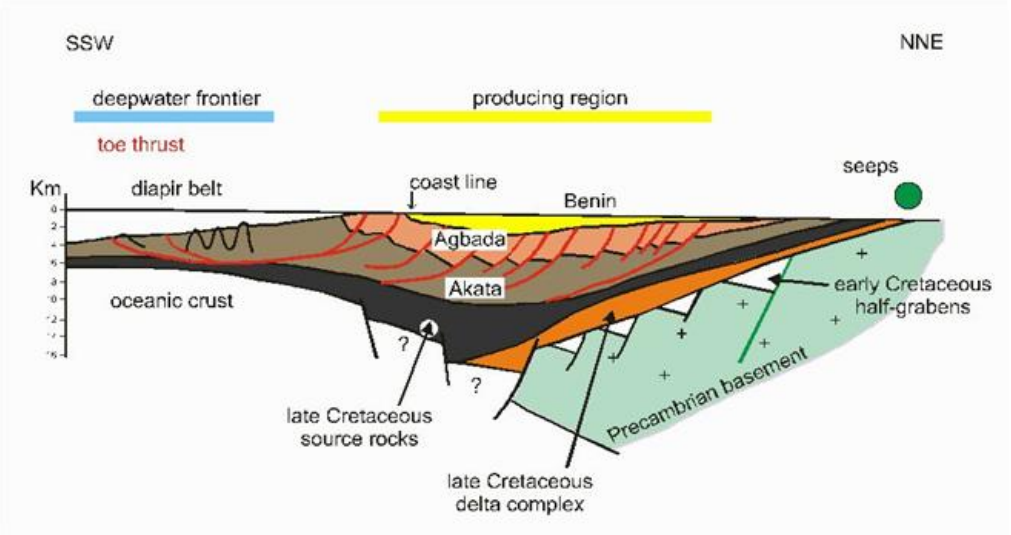

Figure 2. Generalized dip section of the Niger Delta showing the structural styles of the Delta (modified from Thomas, 1995)

2.1. Mechanism of Over-Pressure Generation and Distribution in the Niger Delta Basin

The generation of overpressure and the rate at which it builds up is a function of mechanical mechanisms driving or generating it. Many basins of the world have been reported to be overpressured due to causes such as hydrocarbon expulsion, migration, and entrapment, but there is no known universal relationship between overpressure and hydrocarbon traps (Swarbrick and Osborne 1998; Hunt 1990; Law and Spencer 1998). Authors such as Anowai et. al (2003) and Chopra and Huffman, (2006), attributed different causes of overpressure mechanism but related the main ones to an increase in effective stress and in-situ fluid generating mechanism. Although, disequilibrium compaction has been linked as the primary mechanism of overpressures in most Tertiary basins like the Niger Delta Basin, with the unloading mechanism contributing greatly at depths.

According to Nwaozor et. al., (2013), the onset of overpressures in the Niger Delta basin varied widely between 4494 ft (1370m) tvdss to 14,006 ft (4270m) tvdss with a very diffuse trend in spatial distribution, thereby making isobar maps irrelevant for pore pressure prediction. Later, Anowai et. al (2003) showed that most top of overpressure in the basin is relatively shallower in the Northern and Greater Ugheli Depobelts when compared with the Central Swamp Depobelt and other near-to-offshore fault-bounded megastructures. These trends are accompanied by both shaliness and rate of subsidence where a net–to–gross ratio drops below 35% – 20% in proximity to discontinuous or detached reservoirs such as beaches and channel sands (Anowai et. al., 2003). Until recently, under-compaction has been taken as the mechanism responsible for overpressure generation in Niger Delta. Meanwhile, other factors have been related to the causes of overpressure in the basin (Nwozor et. al., 2013; Opara et. al., 2009; Okocha et. al., 2020). A review of the mechanisms, and the relationship between the causes of overpressure especially as applied to drilling into overpressured reservoirs, is provided by Zijian et. al., (2015).

3. Study Area (Proposed HPHT Deep Exploration Well, Onshore-Shelf, Niger Delta Basin)

Kulon Field was discovered in 1961 in the Central Swamp depobelt (Fig. 3). The field has over twenty-six (26) wells drilled to date across several faults, with most of the wells cutting across eleven reservoirs of interest (with a high net-to-gross ratio). The hydrocarbon type ranges from oil, gas, and non-associated gas (NAG). The proposed Kulon XII Deep well is an untested objective reservoir with several productive and non-productive wells located in its vicinity.

3.1. Data Set and Methods

The data set used in this study is made of wireline log suites (Caliper, Gamma Ray, Density, Neutron, and Resistivity logs), pressure data (measured from permeable aquifers (RCI)), Leak off test (LOT), Mud weights, well directional survey, and seismic velocity volume. Typically, during pore pressure prediction, the emphasis is placed on low permeability interval (shale), this study uses pressure data in sandstone, and further analysis is needed to estimate the formation pressure in shale. Log suites such as gamma-ray, density, and velocity logs were filtered and conditioned using a Gaussian filter to despike unnecessary errors before

loading into ROKDOC software for project mapping in space following the workflow shown in Fig. 4.

3.1.1. *Nomenclatures and Concepts of Pore Pressure and Overburden Pressure (Stress)*

Successful drilling campaign requires accurate use of data to formulate and predict possible down time events. Building a robust geomechanical and geological model will impact helpful communication of risk to forecast drilling hazard during any drilling program. According to Zhang (2011), pore pressures can be defined as fluid pressures occupying the pore spaces in a formation. It is believed that when pore pressure is lower than the hydrostatic pressure (normal pore pressure), it is abnormal pore pressure; when it exceeds the normal pressure, it is overpressure. Pore pressure varies from hydrostatic pressure to severe overpressure (48% to 95% of the overburden stress). Although, there are many causes of over pressure as shown Fig. 5, most prediction models only predict pore pressure generated by stress-related mechanisms (Table 1). The concept of pore pressure prediction was started by Hottmann and Johnson (1965) on shale properties that were derived from sonic and resistivity data and later was modified by Gardner et al., (1974) as shown in Eq. (1).

$$P_f = \sigma_V - \frac{(\alpha_V - \beta)(A_1 - B_1 In\Delta t)^3}{Z^2} \quad (1)$$

where P_f is the formation fluid pressure (psi); σ_V is expressed in psi; α_V is the normal overburden stress gradient (psi/ft); β is the normal fluid pressure gradient (psi/ft); Z is the depth (ft); Δt is the sonic transit time (μs/ft); A and B are the constants, A_1 = 82776 and B_1 =15695. However, in recent times, the fundamental theory for pore pressure prediction is based on many empirical equations like those adopted in this work. However, Terzaghi's equation is believed to be the basic theory for connecting pore pressure with dependent factors. This equation states that if the vertical overburden stress, S increases with depth, Z and there is compaction disequilibrium at a certain depth, the pore pressure, P_P must also increase starting in that depth (Terzaghi et al., 1996). Pore pressure, P_P can be expressed in the following form,

$$P_P = S - \sigma_e \quad (2)$$

Where: P_P = Pore fluid pressure; S = Vertical overburden stress; σ_e = Effective stress.

The pore pressure can be calculated from Eq. (2) if overburden and effective stresses are known. The overburden stress is the combined weight of the rock matrix and fluids in the pore spaces overlying the formation at a specific depth; this can be determined by the integral of bulk density of the sediments using the expression below:

$$S = g\int_0^z \rho b(z)dz = \sum_i^n \rho_b g[Z_i - Z_{i-1}] \quad (3)$$

Where: ρ_b = Depth dependent bulk density due to mechanical compaction; Z_i = Specific depth; Z_{i-1} = Specific depth before i; g = Acceleration due to gravity.

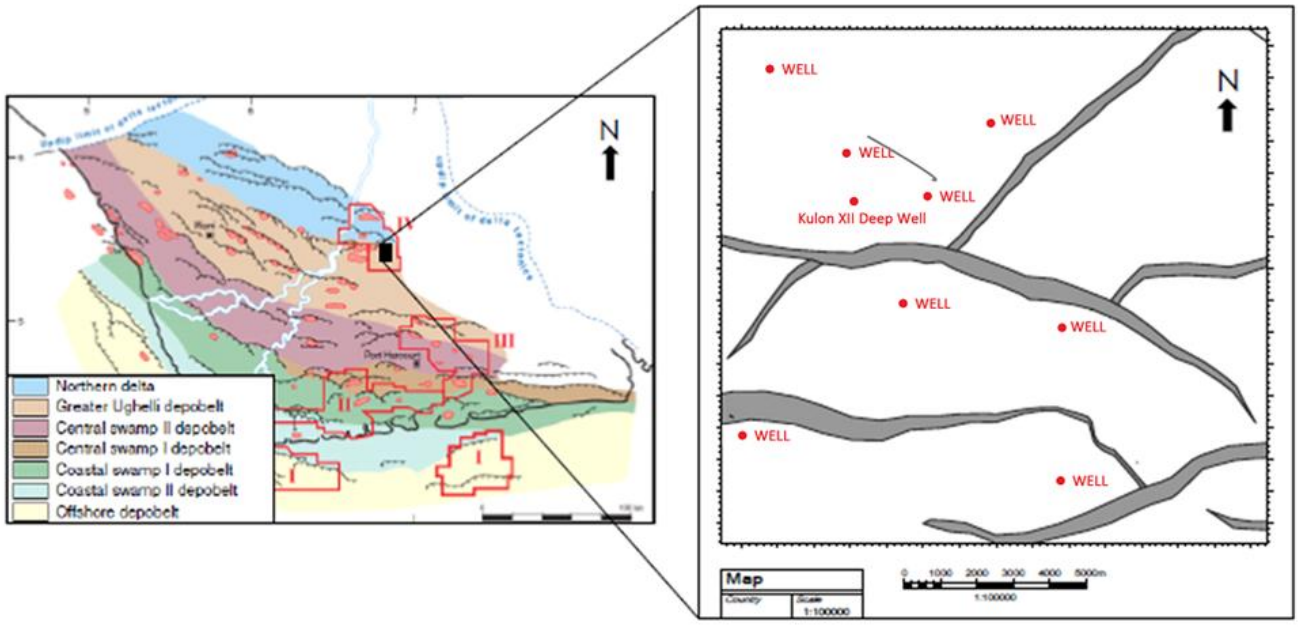

Figure 3. Niger Delta Basin view showing the position of the study area. Insert Proposed Kulon XII Deep well and other well distributions across different fault blocks

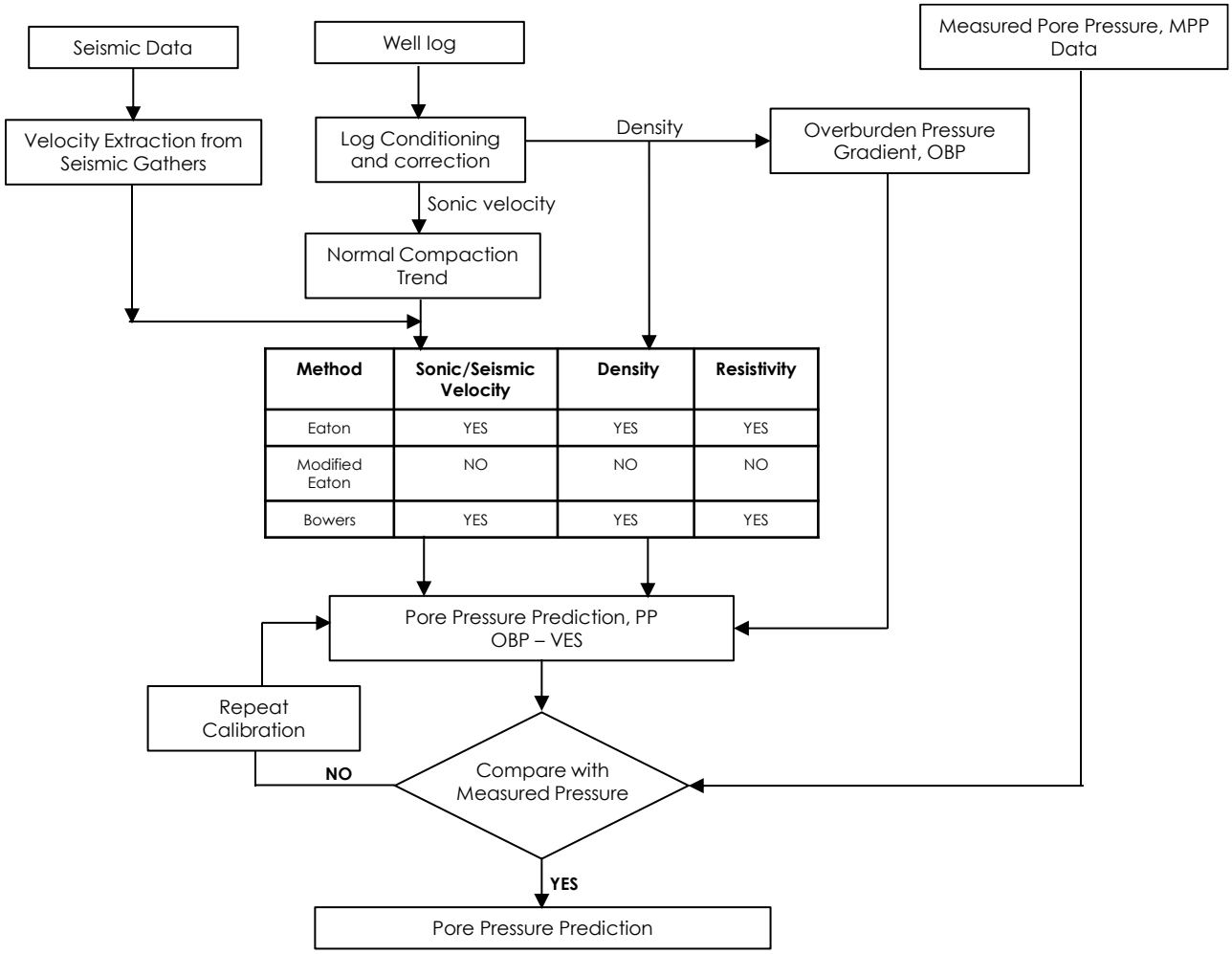

Figure 4. Workflow and methods used for the study

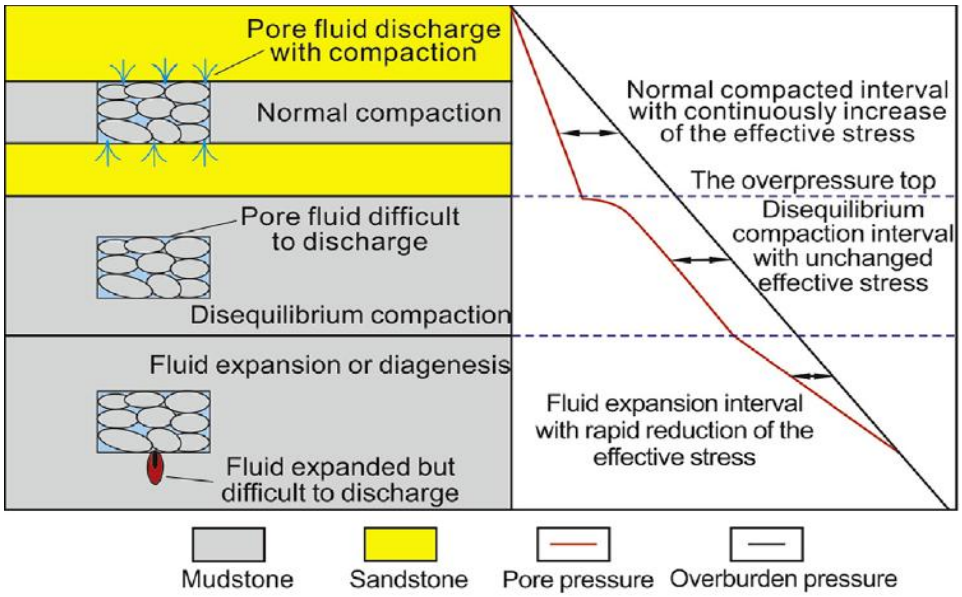

Figure 5. Overview of Pore pressure-causing mechanisms showing the depth of different overpressure mechanisms with their effective stress response (Modified from Bowers, 2011)

10.57647/ijes.2025.16945

In this study, the formation overburden stress was estimated using the deepest well closer to the proposed Kulon XII well. The aim was to determine the overburden pressure gradient, OBP which is fixed in Terzaghi's equation as a proxy for maximum principal stress to relate effective stress and pore pressure.
The formation overburden stress was generated by using the density (ρ) fit model as shown below:

$$\rho_{zml} = \left(\rho_{Matrix} - \rho_{Top}\right)e^{-b(zml)} \quad (4)$$

Where: $\rho_{(zml)}$ = density at depth z below mud line; ρ_{Matrix} = matrix density; ρ_{Top} = density at mud line (seabed) and b is the compaction coefficient.

3.1.2. *Normal Compaction Trend Estimation (NCT)*

It is commonly accepted that porosity decreases exponentially as depth increases in normally compacted formations (Athy, 1930). The normal compaction trend (NCT) of any formation explains the loss of porosity during compaction as sediment burial increases. This step is necessary because, on a velocity–depth plot, velocity should increase symmetrically with depth as a result of compaction. In case of a deviation observed from the trend, overpressure is related as the cause. Normal compaction trend was generated using velocity log within clean shale as input log data and shale cutoff of Vsh ≥ 60%. This trend is estimated using the reciprocal input log transform given by this expression.

$$\frac{1}{V_{p(zml)}} = \frac{1}{V_{pMatrix}} - \left(\frac{1}{V_{pMatrix}} - \frac{1}{V_{pTop}}\right)e^{-b(zml)} \quad (5)$$

Where: $V_{p_{(Matrix)}}$ = Matrix velocity, $V_{p_{(top)}}$ = surface velocity value and b is the value that determines the rate compaction coefficient.

3.1.3. *Filtered Shale Velocity Trend, Vp, and Velocity–Density Crossplot*

As part of data quality control, gamma-ray, density, and sonic velocity logs were filtered to the frequency of 30Hz to improve the data reliability. Velocity values across shale lithology were picked especially where the volume of shale is above 0.5 and was passed into the chimera filter, which applies a Kalman filter to provide estimates of unknown shale values within the cleanest shale to fit a compaction trend (Fig. 6a). Thereafter, Hoesni's Vp – density (Hoesni, 2004), cross-plot approach instead of Bowers Vp – effective stress (Bowers, 1994), cross-plot approach was used to understand the mechanism of overpressure in the field as demonstrated in Fig. 6b. This is because effective stress cannot be measured directly in the field, and a certain percentage of error could have been introduced by the calculation process.

3.1.4. *Velocity Analysis and Well Data Calibration*

Seismic velocity analysis is an important step in pore pressure prediction analysis. Generally, it is performed to account for the moveout in reflection time with offset (Yilmaz and Doherty, 2000). In geopressure prediction, seismic velocity analysis is aimed at detecting abrupt changes in velocities which are determined after processing common midpoint (CMP) gathers to get true formation velocity as shown in Fig. 7. Sometimes it is determined by best-fitting normal moveout velocity (V_{nmo}) as a function of vertical two-way time for each major reflector. To ensure accuracy, considerations are based on the velocities that flatten the reflector at zero offsets as shown in Fig. 7b. The Dix linear relationship was used to generate the interval velocities (V_{int}) that were used to flatten the reflector at zero offsets. A relationship between velocities and pore pressure was established using offset well data. This enables reliability tests on the acoustic parameters from wells, to determine the formation pressure ahead of drilling as well as eliminate errors in the velocities due to domain shift. The error elimination was done by fitting polynomial functions to derive calibrated seismic velocity using the relationship shown in Equation 6 below:

$$V_{int} = V_0 + K_z \quad (6)$$

Where: Vint = Interval velocity; V_0 is the assumed velocity at the near-surface; K_z is velocity gradient in ft/sec/ft or 1/sec and Z, is depth in ft or m.
This established relationship was used to predict formation pressure ahead of drilling. The accuracy of the relationship is based on the availability of measured pressure data to logged depth, which serves as a calibrating standard.

3.2. Review of Eaton's and Bowers' Pore Pressure Prediction

3.2.1. *Eaton's Method*

The Eaton method is mainly applied in young sedimentary basins where under-compaction is the major cause of overpressure (Zhang, 2011). The Eaton method does not consider unloading mechanical mechanism and is based on certain assumptions such as that rocks are mechanically compacted; sediments are at maximum effective stress; lithology is thick shale; and normal compaction trend can be defined (based on the fact that only mechanical compaction has operated and rocks are presently at their maximum effective stress).

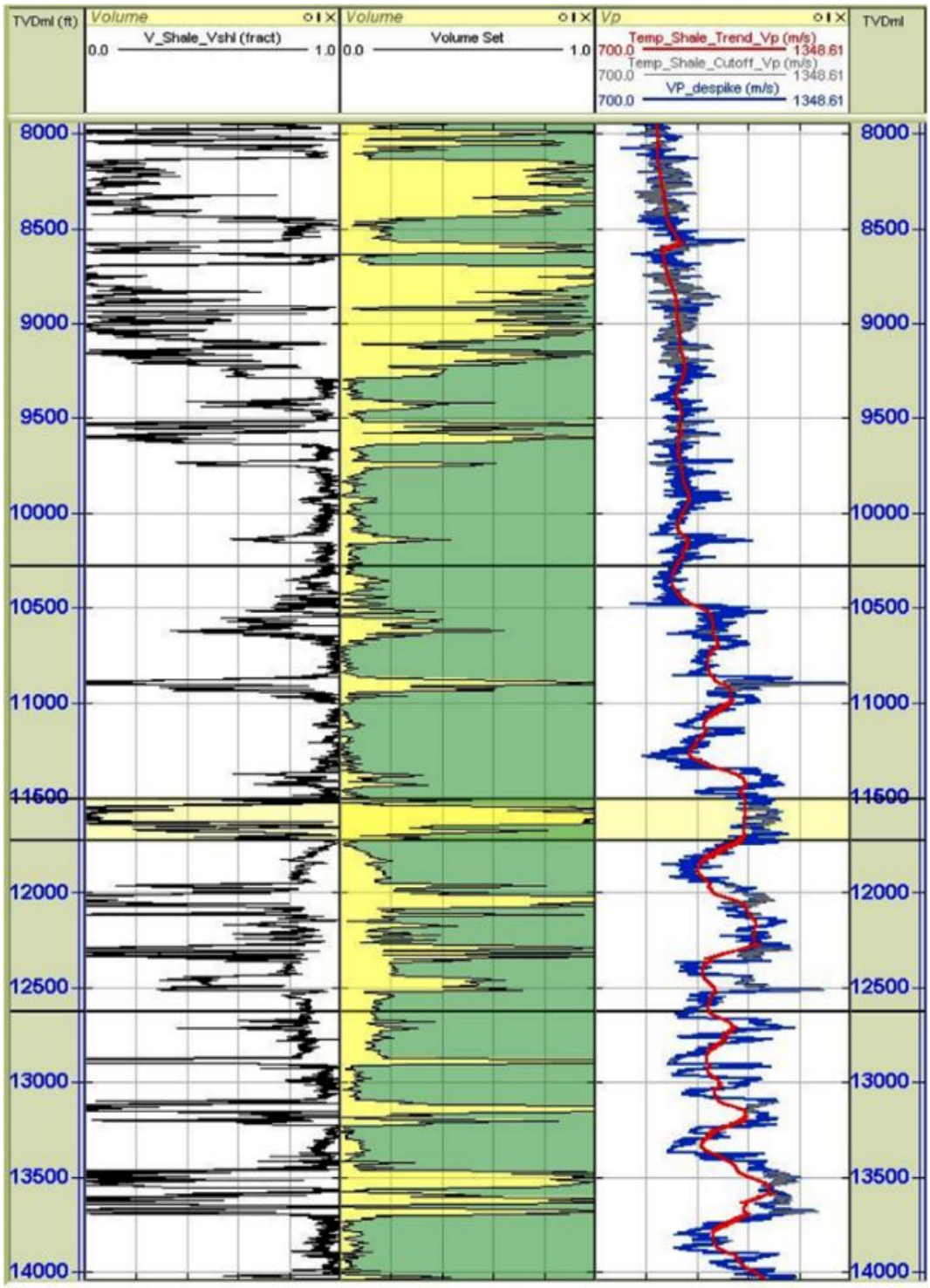

Figure 6a. Shale Vp trend after applying Kalman filtering (Track 3)

It critically depends on the fact that different lithologies compact at different rates, and from contrasting starting porosity. This shows that the occurrence of pore pressure in any formation is a function of total stress (or overburden stress) and effective stress (Biot, 1941). Empirical equations for predicting pore pressure prediction were established by (Eaton, 1972; Eaton, 1975). Eaton related effective stress with the effective stress of a normally compacted formation, the velocity of a normally compacted formation, and the measured velocity. The expression can be related by

$$\sigma = \sigma_n \left(\frac{V}{V_n}\right)^3 \quad (7)$$

where σ = effective stress, σ_n = effective stress of a normally compacted formation, V_n = velocity of a normally

10.57647/ijes.2025.16945

compacted formation, and V = observed velocity. Applying equation (7) to Terzhagi's approach will generate an expression for pore pressure gradient using sonic compressional transit time and resistivity log.

$$P_p = S_v - (S_v - P_n)\left(\frac{\Delta t_{norm}}{\Delta t_{obs}}\right)^x \quad (8a)$$

$$P_p = S_v - (S_v - P_n)\left(\frac{V_{pobs}}{V_{pnorm}}\right)^x \quad (8b)$$

$$P_p = P_{ovb} - (P_{ovb} - P_n)\left(\frac{R}{R_n}\right)^{1.2} \quad (9)$$

Where P_p = Pore pressure gradient; P_{ovb} = Overburden stress gradient; P_n = Hydrostatic pore pressure gradient (normally 0.45 psi/ft or 1.03 MPa/km, dependent on water gradient salinity); R = Shale resistivity from the log; R_n = Shale resistivity at the normal (hydrostatic) pressure;

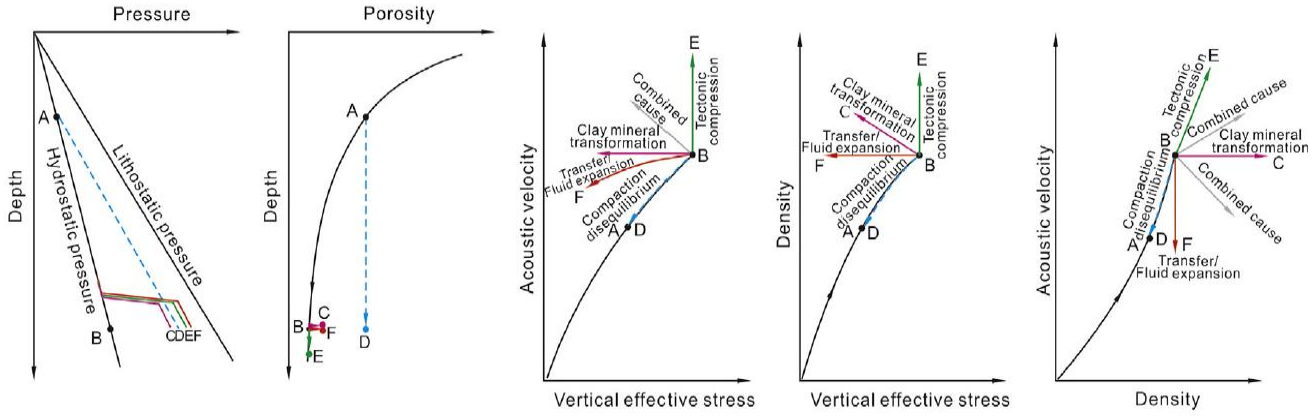

Figure 6. Relationship between vertical effective stress and acoustic velocity/density of different overpressuring mechanisms and the acoustic velocity-density cross plots. **"A"** is the equivalent depth of compaction disequilibrium. **"B"** is the normal compaction/normal pressure. **"C"** represents the overpressure caused by clay mineral transformation. **"D"** represents the overpressure caused by disequilibrium compaction. **"E"** represents the overpressure caused by tectonic compression. **"F"** represents the overpressure caused by fluid expansion (hydrocarbon generation)/pressure transfer (After Zhao et. al., 2018)

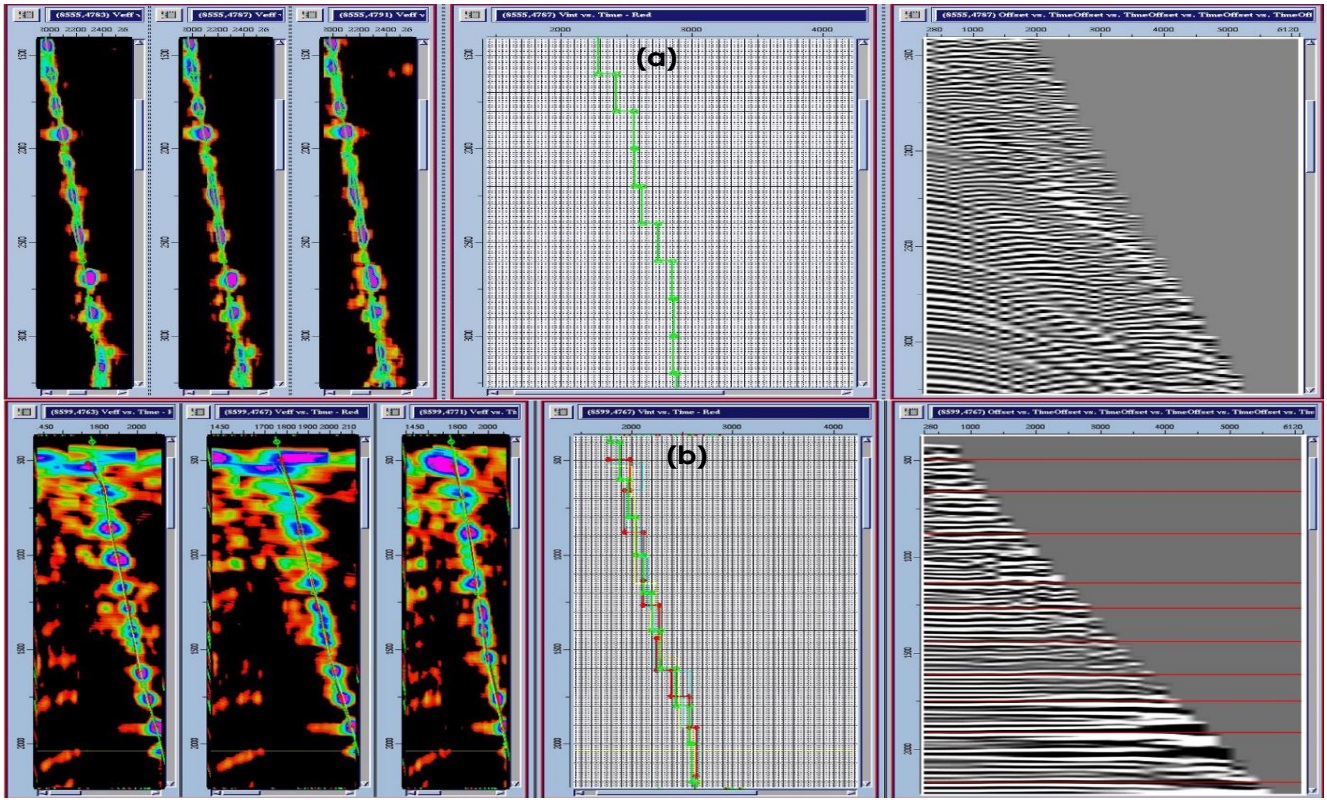

Figure 7. Common Mid-Point Gathers, CMP (a) Before velocity picking (b) After velocity picking showing flattened reflectors

10.57647/ijes.2025.16945

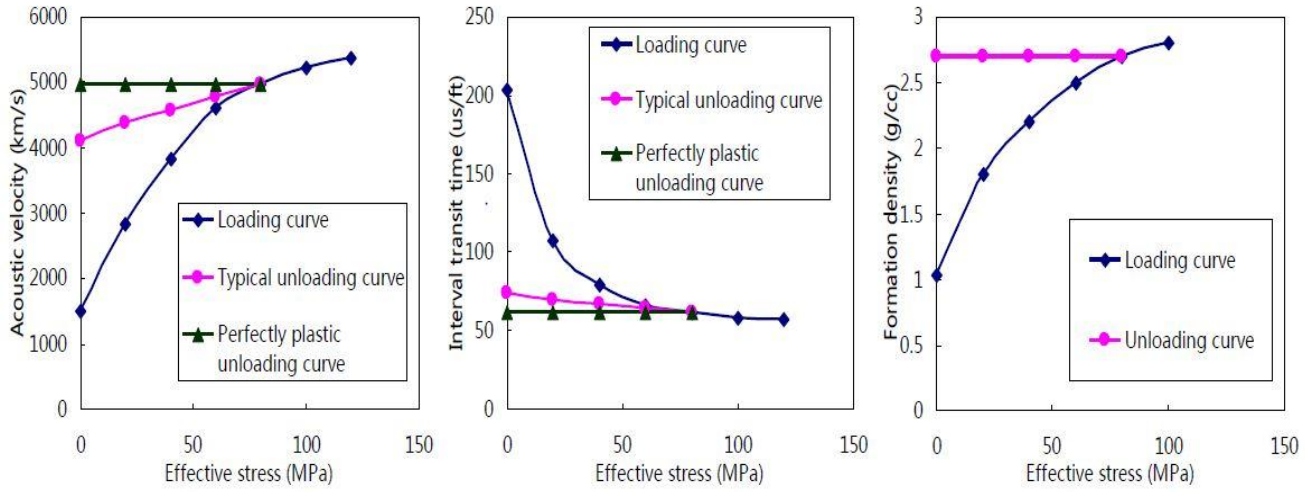

Figure 8. Behaviour of logging data during the loading and unloading of shale. (Modified from Zijian, 2015)

Δt_{norm} = Sonic transit time or slowness in shales at the normal pressure; Δt_{obs} = Sonic transit time in shales from the log, and can be derived from seismic interval velocity; Vp_{obs} = velocity observed; and Vp_{norm} = velocity on normal trend; the x exponential constant was taken to be 3 for overpressure caused by disequilibrium compaction.

3.2.2. *Bowers' Method*

The origin of overpressures can be determined through the use of Bowers (1994), porosity-vertical effective stress chart, popularly known as the loading-unloading curve. To determine overpressures caused by unloading, it is necessary to make both the effective stress-velocity relation diagram and the effective stress-density relation diagram when compiling loading-unloading curve charts (Bowers 1994). In Fig. 8, overpressures caused by disequilibrium compaction were plotted on the loading curve, while those caused by fluid expansion were plotted on the unloading curve. However, an observed reversal could be a result of a change in lithology (change in velocity) not necessarily associated with pore pressure. Bowers (1994), proposed a relationship that relates pore pressure with measured velocity and the velocity at the mud line and used the relationship to account for excess pressure generated by both under-compaction and fluid expansion mechanisms. Effective stress was calculated from velocity without having to establish a compaction trend and subtracted the result from the overburden stress to obtain pore pressure using Equation (10).

$$\sigma_e = \sigma_v - P_p \quad (10a)$$

Where: σ_e = Effective Stress; σ_v = overburden stress; P_p = Pore Pressure.

He proposed that the sonic velocity and effective stress have a power relationship as follows:

$$V_p = V_{ml} + A{\sigma_e}^B \quad (10b)$$

V_p = the compressional velocity at a given depth; V_{ml} = the compressional velocity in the mud line (i.e. the sea floor or the ground surface, normally $V_{ml} \approx 5000$ft/s or 1520 m/s); A and B are the parameters calibrated with offset velocity versus effective stress data.
Rearranging Equation (10b) the pore pressure can be obtained from the velocity as described in Equation (10a):

$$P_p = \sigma_v - \left(\frac{V_p - V_{ml}}{A}\right)^{\frac{1}{B}} \quad (11)$$

For example, regional parameters for Niger Delta wells, A = 8 and B = 0.57 in the English units (P_p, σ_v, in Psi and V_p, V_{ml} in ft/s).

4. Results and Discussion

4.1. Overburden Pressure and Normal Compaction Trend (NCT)

The overburden pressure gradient derived from the density log of the deepest well-plotted parallel to the gradient generated at a fixed gradient of 1.03 psi/ft as shown in Fig. 9a. The density log calculation showed that the overburden gradient ranges from 0.78 to 0.96 psi/ft. The red line in Fig. 9a is the estimated overburden gradient from the density log, showing the error margin of the density log (Rho) and the Rho fit in the dotted line. The black line in Figure 9b represents the overburden pressure of a fixed gradient. Meanwhile, the trend fit the sonic velocity (Fig. 9c), shows

a pronounced compaction gradient that increases at a fast rate within the shallow depth and slows down at greater depth. Also, Fig. 9c shows that sediment compaction was normal until the depth of 10,300 ft. (TVDml) where the onset of overpressure is assumed. The stratigraphic correlation of wells in the Kulon field shows that the overpressure onset corresponds with the 15.0 myr MFS (Bolivina 25 Maximum Flooding Surface), which suggests it is the sealing boundary that acts as a blanket preventing the total expulsion of pore fluid.

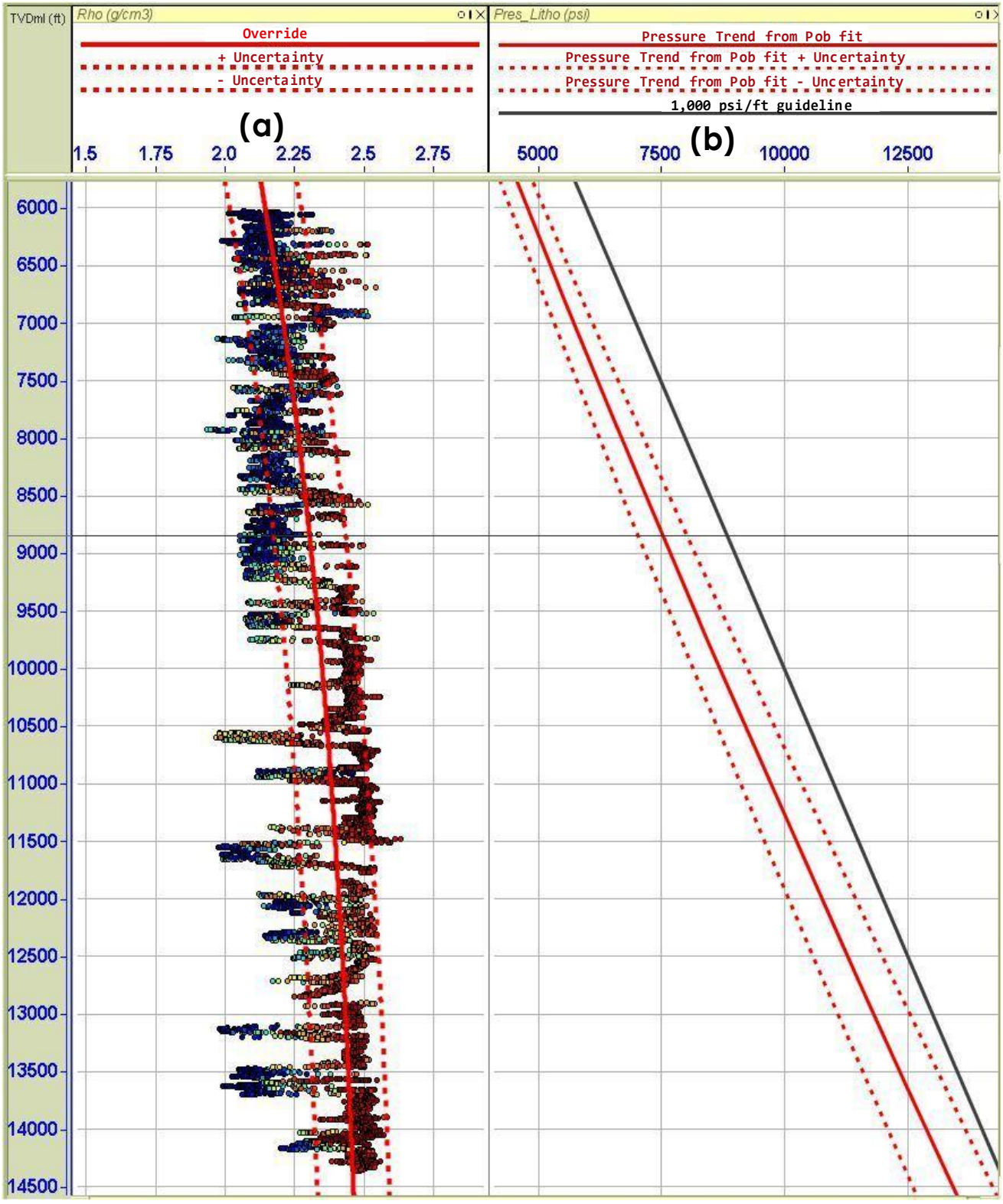

Figure 9 (a-b). Overburden Pressure from the deepest well in the Kulon Field **(a)** density log (Rho) and the Rho fit **(b)** Overburden pressure of a fixed gradient (Blackline), while the red line is the estimated overburden gradient from density log with the error margin in dotted line

10.57647/ijes.2025.16945

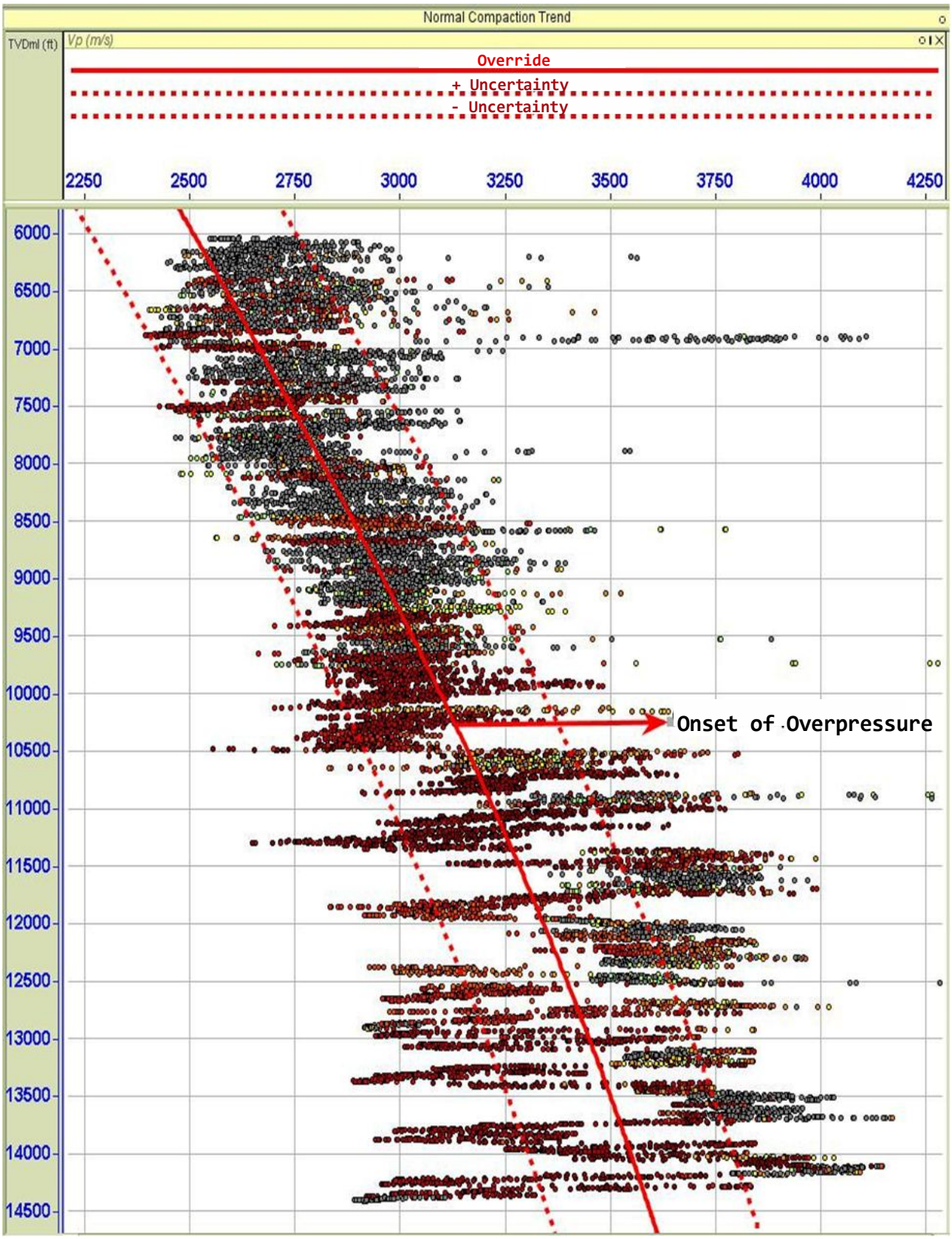

Figure 9c. Overburden Pressure from the deepest well in the Kulon field showing sonic velocity generated Normal Compaction Trend (NCT). **Note**: The greyed-out points on the plot are intervals with sand

10.57647/ijes.2025.16945

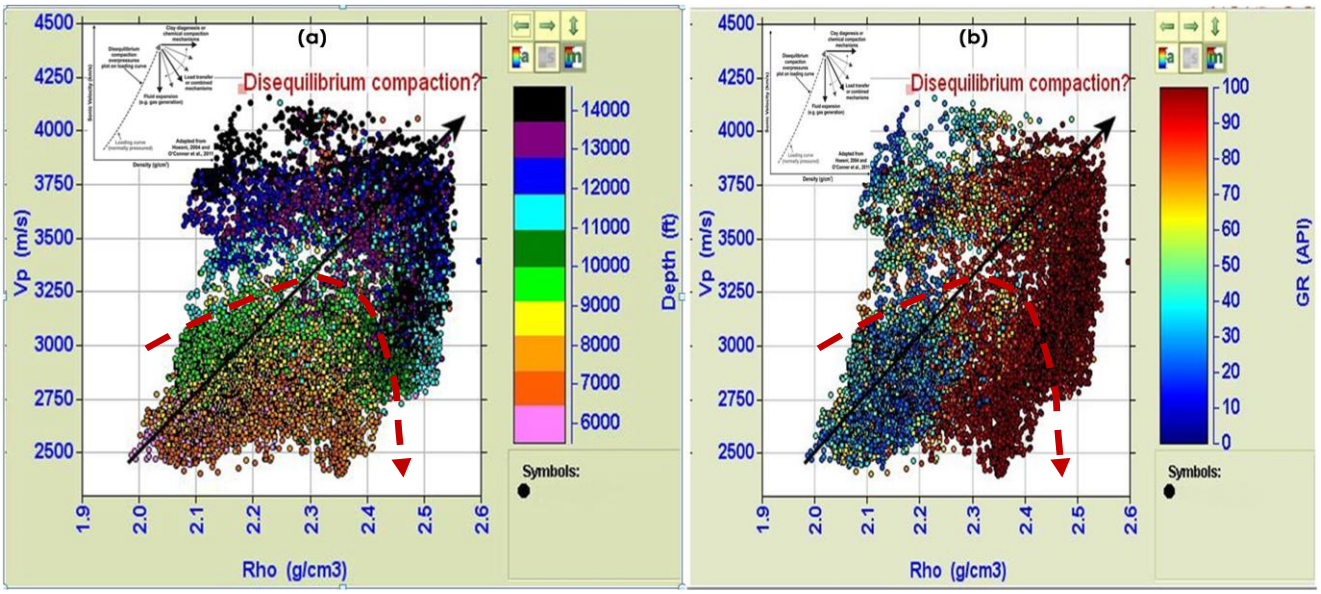

Figure 10. Velocity–density cross plot from the deepest well in the Kulon Field **(a)** coloured in-depth values **(b)** coloured in gamma-ray values with shale cutoff of 0.5. **Note:** The dotted red line shows the inferred onset of overpressure and reversal of velocity and density values of shale with depth

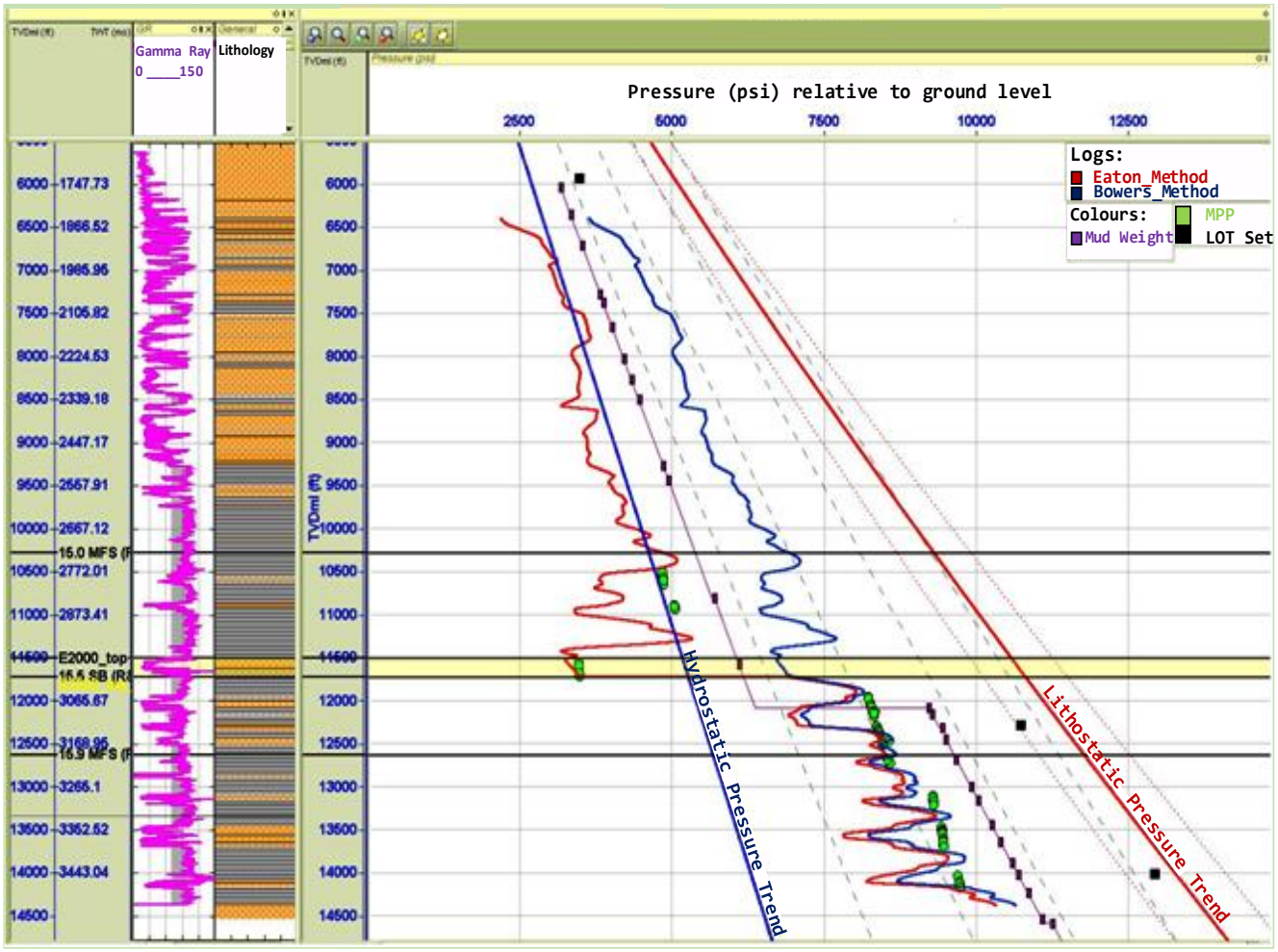

Figure 11. Offset well pore pressure prediction model using the closest well for the proposed Kulon XII deep well

10.57647/ijes.2025.16945

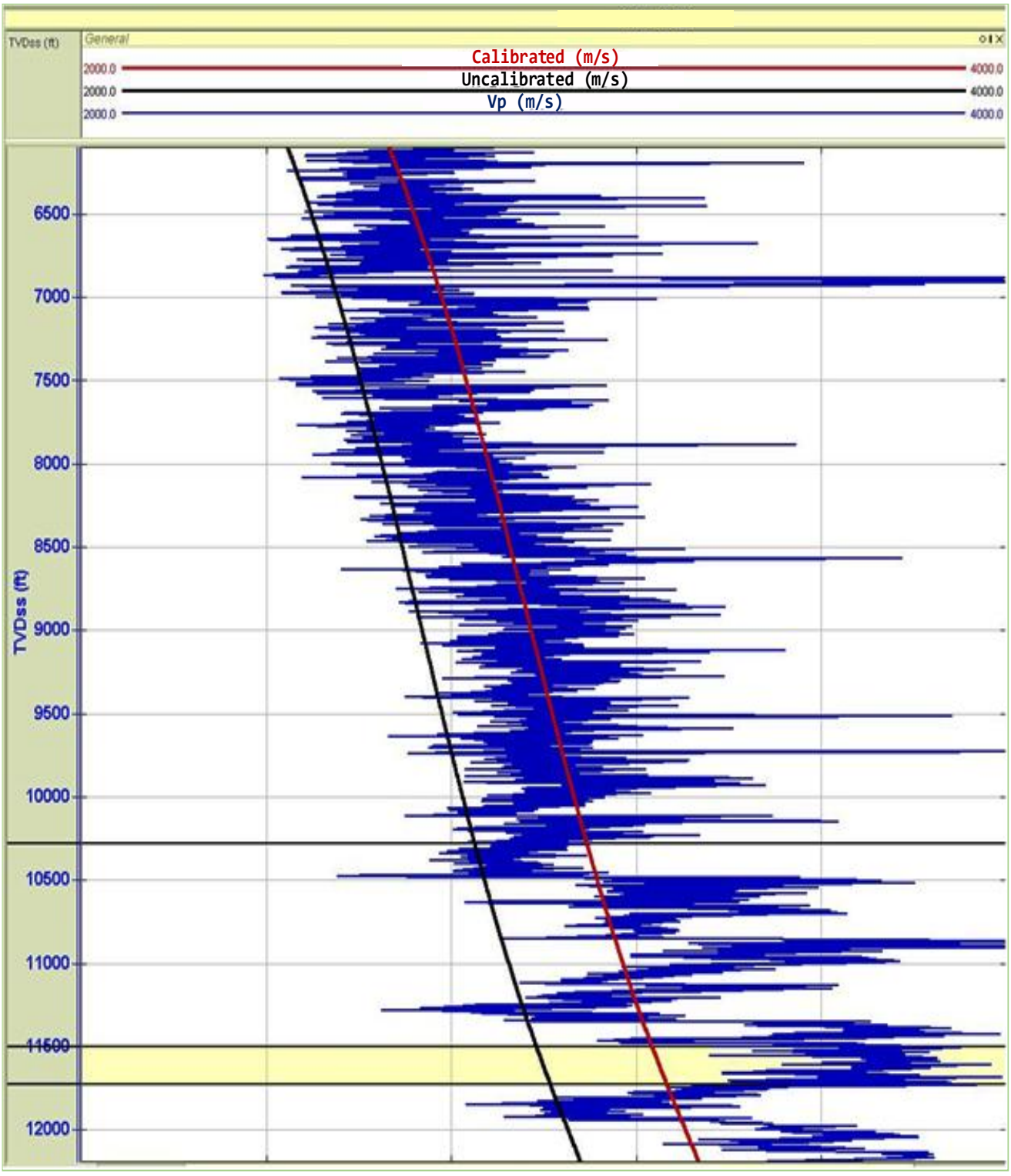

Figure 12. Seismic to well calibration. (i) Blackline is the un-calibrated seismic velocity; the red line is the calibrated velocity and the blue wiggle is the compressional velocity

4.2. Hoesni Cross Plot of Velocity – Density

The Hoesni cross plots of compressional velocity, Vp, and density, Rho suggests disequilibrium compaction as the mechanism responsible for the overpressures (Fig. 10). The plot showed a sharp increase in density gradient at a shallow depth of about 10,300ft which corresponds with the 15.0 myr MFS (Bolivina 25 Maximum Flooding Surface) which is the onset of overpressure (as shown in Fig 9c).

10.57647/ijes.2025.16945

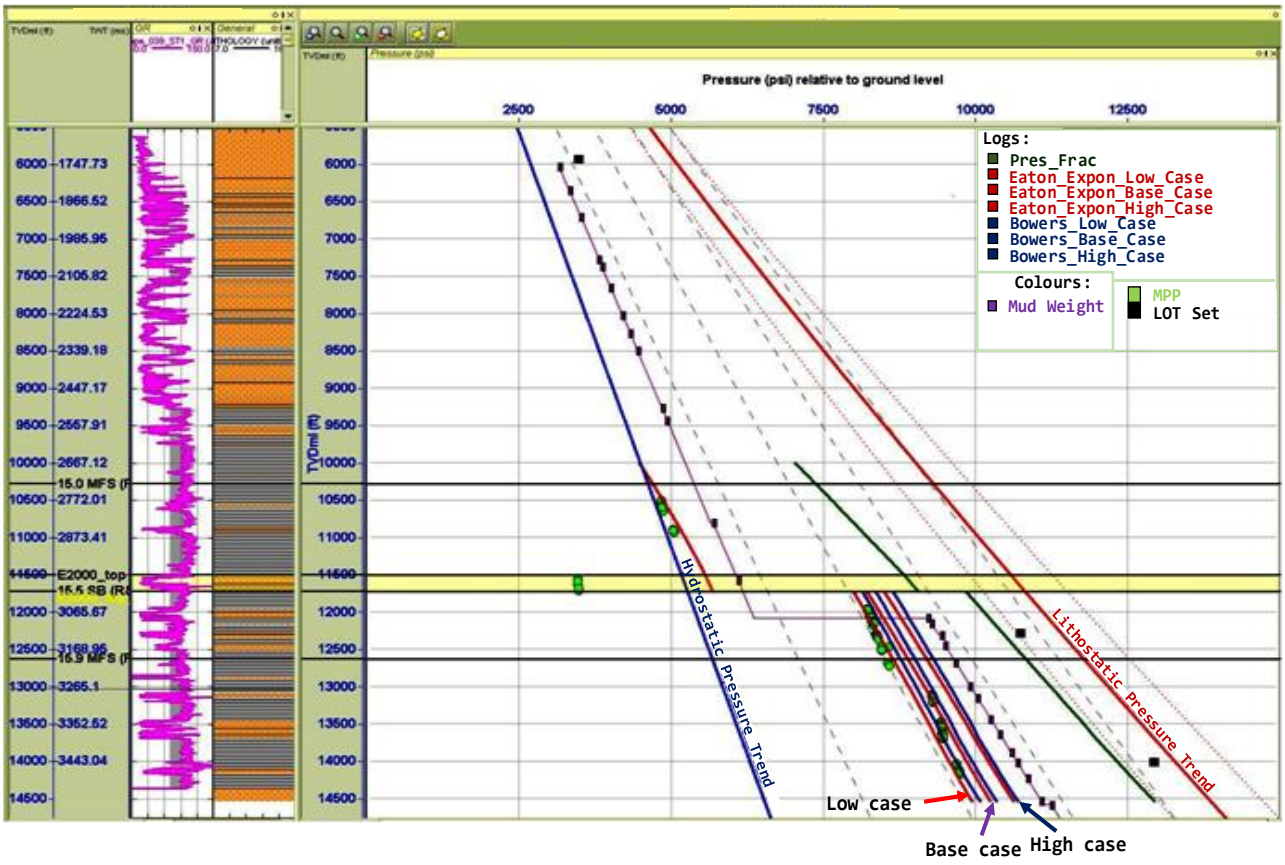

Figure 13. Seismic pore pressure prediction for offset well (Low case, Base case and High case)

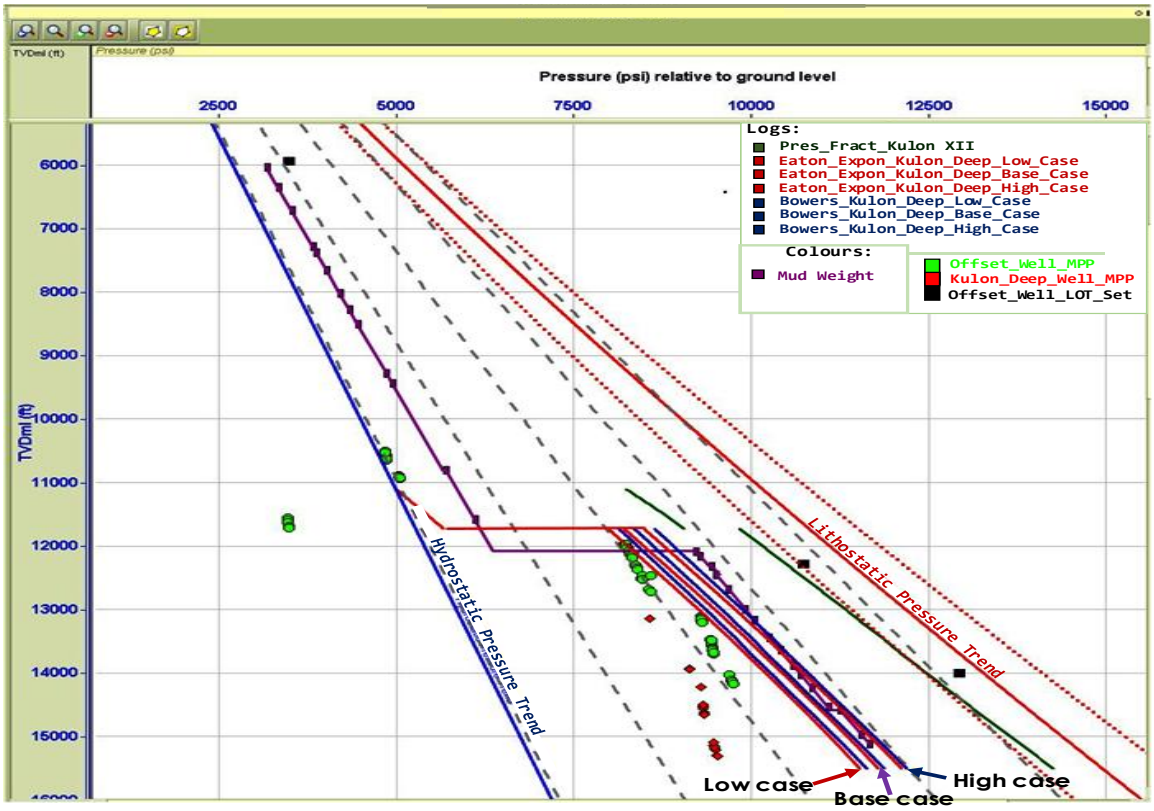

Figure 14. Seismic pore pressure prediction for Kulon XII Deep Well (Low case, Base case and High case)

10.57647/ijes.2025.16945

The velocity/density gradient changed from that depth onward showing further pronounced reversal in velocity and density values (Fig. 10a). The onset of overpressure which was inferred from changes in velocity/density gradient falls within the shale interval (as shown in Figure 10b). This confirms that the fluid retention at that depth is a result of a rapid influx of low permeability sediments during and within 15.0 myrs sediment deposition.

4.3. Pore Pressure Prediction from the Offset Well

The prediction of pore pressure for the closest well to Kulon XII deep well showed the assumed exponential constant in Equs. (8) gave a pressure profile that aligned closely with the measured pressures after 11,750ft. Between depths 11,500ft – 11,750ft, Eaton's prediction model occurred below the hydrostatic gradient as shown in Fig. 11. This is a result of production depletion as there is no evidence of overpressuring due to lateral drainage in any of the wells within the same fault block as all faults bounding the fault block are sealing faults. Results using the Bowers method showed that at the shallow depth, the method gave an estimate of pressure greater than the required mud weight used during drilling. This implies that the method overestimated pore pressure at shallow depths (Fig. 11). The implication is that the mudline velocity which will give a good match with the mud weight at shallow depth, does not calibrate with measured pressure at greater depth. At this point, the Bowers method was not considered for shallow depth for the proposed Kulon XII well. The observations made from the predicted models of Eatons and Bowers at depths greater than 12,000ft showed an aligned pattern closer to the measured pore pressure, therefore both models were considered for deeper depth for the proposed well.

4.4. Seismic Pore Pressure Prediction for the Offset Well and Kolon XII Deep Exploration Well

The calibration between the well and seismic showed that the profile line of the seismic velocity before calibration did not match the velocity log average trend line. After calibration, the seismic velocity aligned with the average trend of the velocity logs as confirmation of the best fit for pore pressure prediction (Fig. 12). The Eatons and Bowers derived pore pressure relationship for the offset well using offset sonic velocity was used to generate a pore pressure profile that reliably calibrated with the measured data as shown in Fig. 13. The pore pressure profile indicated that the offset well experienced mild overpressure at a depth of 11,900ft with no record of hard overpressure in the well.
This increased the level of confidence as the velocity was scaled on a factor of +/- 5% of the raw seismic velocity. The implication remains that the seismic velocity and the prediction models remain reliable for pore pressure prediction in the proposed deep exploratory well that has no log data. The result of the pressure prediction transform from the offset well was applied to the proposed Kulon XII deep exploration well. The proposed pressure profile indicated the onset of overpressure at a depth deeper than 11,900ft as observed in the offset well in Fig. 13. After scaling the velocity by a factor of +/- 5%, the result of the predicted pressure showed that a higher mud weight will be required for drilling the Kulon XII deep well, in order not to experience kick at greater depth. The result of Kulon XII deep pressure prediction (Fig. 14) gave an estimate of the expected pressure to be above 13,000ft.

5. Conclusion

Understanding the causes of abnormal or overpressure mechanisms is key to a successful drilling campaign. Based on this study, overpressure in the Kulon field is caused by compaction disequilibrium. This was identified using the Hoesni velocity and density cross-plotting approach. The cross plot identified the low permeability 15.0Ma MFS sequence (Bolivina 25 Maximum Flooding Surface) as the overpressure sequence. The pore pressure prediction using the offset well closest to the proposed Kulon XII well especially at depths less than 11,750ft (shallow depth) shows that Eaton's model predicted pore pressure below hydrostatic gradient, while Bowers model at the same condition overestimated pore pressures. This uncertainty observed from Bower's prediction model was not considered for pore pressure prediction of the proposed Kulon XII deep well. Also, uncertainties in Eaton and Bowers's prediction model at the shallow interval were attributed to production depletion at shallow depth (less than 11,750ft) and better mud line velocity calibration with the mud weight at a depth above 11,750ft (deeper depth). At depths greater than 12,000ft, the Eaton and Bowers prediction model showed a closer match with the measured pore pressure as a result was used for pore pressure prediction at deeper intervals of the proposed well. The predicted pore pressure profile from the offset well indicated the well was mildly overpressured at depths greater than 11,900ft. Although the pressure regime and the onset of overpressure in the offset well are known, the Kulon XII deep well pressure was predicted at 13,000ft, higher mud weight will be required for optimum production and a safer drilling campaign at greater depth.

Acknowledgment

The authors wish to thank the University Liaison Unit of Shell Petroleum Development Company (SPDC), Port Harcourt; the University of Nigeria, Nsukka (UNN) for the provision of datasets, research opportunities, and enabling conditions to carry out this research work. Our sincere

appreciation goes to Glenn Bowers for his professional advice and contribution during this study in SPDC.

Authors Contribution
All the authors have participated sufficiently in the intellectual content, conception, and design of this work or the analysis and interpretation of the data (when applicable), as well as the writing of the manuscript.

Availability of data and materials
The data that support the findings of this study are available from the corresponding author upon reasonable request.

Conflict of interest
The author states that there is no conflict of interest.

References

Anowai, C.A., Ejadawe, J.E. and Adeoye, S.S. 2003. Regional overpressure study of the Niger Delta using seismic velocities. *EP2003 – 5382*.

Athy, L.F. 1930. Density, porosity, and compaction of sedimentary rocks. *AAPG Bulletin*, 14(1), pp. 1–24. DOI: https://doi.org/10.1306/3d93289e-16b1-11d7-8645000102c1865d

Badri, A.B., Sayers, C.M., Awad, R. and Graziano, A. 2000. A feasibility study for pore-pressure prediction using seismic velocity in offshore Nile Delta, Egypt. *The Leading Edge*, 19(10), pp. 1103–1108. DOI: https://doi.org/10.1190/1.1438487

Biot, M.A. 1941. General theory of three-dimensional consolidation. *Journal of Applied Physics*, 12, pp. 55–164. DOI: https://doi.org/10.1063/1.1712886

Bowers, G.L. 2011. Determining an Appropriate Pore pressure Estimation Strategy. Offshore Technology Conference, Houston. DOI: https://doi.org/10.4043/13042 MS

Bowers, G.L. 1994. Pore pressure estimation from velocity data: Accounting for overpressure mechanisms besides undercompaction. *International Journal of Rock Mechanics and Mining Sciences & Geomechanics Abstracts*. DOI: https://doi.org/10.1016/0148-9062(94)90121-X

Bowers, G.L. 1995. Pore pressure estimation from velocity data: Accounting for overpressure mechanisms besides undercompaction. *SPE Drilling and Completions*, June 1995, pp. 1–19. DOI: https://doi.org/10.2118/27488-PA

Bowers, G.L. 2001. Determining an appropriate pore-pressure estimation strategy. *Offshore Technology Conference*, Houston. DOI: https://doi.org/10.4043/13042-MS

Chopra, S. and Huffman, A. 2006. Velocity Determination for Pore Pressure Prediction. *CSEG Recorder*, 2006, pp. 28–46. DOI: http://dx.doi.org/10.1190/1.2405336

Corredor, F., Shaw, J.H. and Bilotti, F. 2005. Structural styles in the deep-water fold and thrust belts of the Niger Delta. *AAPG Bulletin*, 89, pp. 753–780. DOI: https://doi.org/10.1306/02170504074

Das, G. and Maiti, S. 2024. A machine learning approach for the prediction of pore pressure using well-log data of Hikurangi Tuaheni Zone of IODP Expedition 372, New Zealand. *Energy Geoscience*, 5, 100227. DOI: https://doi.org/10.1016/j.engeos.2023.100227

Dehghan, A.N. and Yazdi, A. 2023. A geomechanical investigation for optimizing the ultimate slope design of Shadan Open Pit Mine, Iran. *Indian Geotechnical Journal*, pp. 1–15. DOI: https://doi.org/10.1007/s40098-022-00709-w

Eaton, B.A. 1972. The effect of overburden stress on geopressure prediction from well logs. *Journal of Petroleum Technology*, SPE 3719. DOI: https://doi.org/10.2118/3719-PA

Eaton, B.A. 1975. The equation for geopressure prediction from well logs. *Society of Petroleum Engineers of AIME*, SPE 5544. DOI: https://doi.org/10.2118/5544-MS

Evamy, B.D., Haremboure, J., Kamerling, P., Knaap, W.A., Molloy, F.A. and Rowlands, P.H. 1978. Hydrocarbon habitat of Tertiary Niger Delta. *Petroleum Geochemistry and Basin Evaluation*. DOI: https://doi.org/10.1306/M35439C19

Gardner, G.H.F., Gardner, L.W. and Gregory, A.R. 1974. Formation Velocity and Density—The Diagnostic Basics for Stratigraphic Traps. Geophysics, 39, pp. 770–780. DOI: http://dx.doi.org/10.1190/1.1440465

Hamid, O., Khan, K., Rahim, Z., Omair, A., Ahmed, S. and Ahmed, M. 2016. Reducing drilling operational risk and non-productive time using real-time geomechanics surveillance. *International Petroleum Technology Conference*. DOI: https://doi.org/10.2523/IPTC-18793-MS

Hoesni, J. 2004. Origins of overpressure in the Malay Basin and its influence on petroleum systems. *University of Durham*, Durham, p. 268.

Holand, P. and Skalle, P. 2001. Deepwater kicks and BOP performance. *SINTEF Report for U.S. Minerals Management Service*.

Hunt, J.M. 1990. Generation and migration of petroleum from abnormally pressured fluid compartments. *AAPG Bulletin*, 74(1), pp. 1–12.

Karimiazar, M., Teshnizi, E.S., O'Kelly, B.C., Sadeghi, S., Karimizad, N., Yazdi, A. and Arjmandzadeh, R. 2023. Effect of nano-silica on engineering properties of lime-treated marl soil. *Transportation Geotechnics*, 43, pp. 101123. DOI: https://doi.org/10.1016/j.trgeo.2023.101123

Law, B.E. and Spencer, C.W. 1998. Abnormal pressures in hydrocarbon environments. In: Law, B.E., Ulmishek, G.F. and Slavin, V.I. (Eds.), Abnormal Pressures in Hydrocarbon Environments, *AAPG, Tulsa*, pp. 1–11. DOI: https://doi.org/10.1306/M70615C1

Lehner, P. and De Ruiter, P.A.C. 1977. Structural history of Atlantic Margin of Africa. *AAPG Bulletin*, 61, pp. 961–981. DOI: https://doi.org/10.1306/c1ea43b0-16c9-11d7-8645000102c1865d

Nwozor, K.R., Omudu, M.I., Ozumba, B.M., Egbuachor, C.J., Onwuemesi, A.G. and Anike, O.I. 2013. Quantitative evidence of secondary mechanisms of overpressure generation: Insights from parts of Onshore Niger Delta, Nigeria. *Journal of Petroleum Technology and Development*, 3(1), pp. 64–83.

Okocha, I.A., Mamah, L.I. and Okeugo, C.G. 2020. Abnormal pore pressure prediction using modified Eaton model: A case of Zeta Field, Onshore-Shelf, Niger Delta Basin. *Petroleum and Coal*, 62(1), pp. 244–254.

Opara, A., Onuoha, K.M., Anowai, C., Mbah, R. and Onu, N.N. 2009. Overpressure and Trap Integrity Studies in Parts of the Niger Delta Basin: Implications for Hydrocarbon Prospectivity. *Nigerian Association of Petroleum Exploration*, 2008.

Osborne, M.J. and Swarbrick, R.E. 1997. Mechanisms for generating overpressure in sedimentary basins: A reevaluation. *AAPG Bulletin*, 81, pp. 1023–1041.

Reijers, T.J.A. 2011. Stratigraphy and sedimentology of the Niger Delta. *Geologos*, 17(3), pp. 133–162. DOI: https://doi.org/10.2478/v10118-011-0008-3

Short, K.C. and Stauble, A.J. 1967. Outline of the geology of the Niger Delta. *American Association of Petroleum Geologists Bulletin*, 51, pp. 761–779. DOI: https://doi.org/10.1306/5d25c0cf-16c1-11d7-8645000102c1865d

Skalle, P. and Podi, A.L. 1998. Trends extracted from 800 Gulf Coast blowouts during 1960–1996. *World Oil*, June 1998, pp. 67–72. DOI: https://doi.org/10.2118/39354-MS

Steve, R.L., Munday, S. and Bray, R. 2002. Regional geology and geophysics of the eastern Gulf of Guinea (Niger Delta to Rio Muni). *The Leading Edge, November*, pp. 1112–1117. DOI: https://doi.org/10.1190/1.1523752

Swarbrick, R.E. and Osborne, M.J. 1998. Mechanisms that generate abnormal pressures: An overview. In: Law, B.E., Ulmishek, G.F. and Slavin, V.I. (Eds.), *Abnormal Pressures in Hydrocarbon Environments*, *AAPG Memoir* 70, pp. 13–34. Tulsa, OK. DOI: https://doi.org/10.1306/M70615C2

Swarbrick, R.E. 1999. Pressure regimes in sedimentary basins and their prediction. *Marine and Petroleum Geology*, 16, pp. 483–486.

Terzaghi, K., Peck, R.B. and Mesri, G. 1996. Soil mechanics in engineering practice (3rd ed.). *John Wiley & Sons*.

Thomas, D. 1995. Exploration gaps exist in Nigeria's prolific Delta. *Oil and Gas Journal*, October 30, pp. 66–71.

Ugbor, C.C., Odofin, D. and Okeugo, C.G. 2026. Reducing Geopressure‐Related Non‐Productive Drilling Downtime: A Case of Recent Proposed HPHT Deep Exploration Well, Onshore‐Shelf, Niger Delta Basin, Nigeria. *Journal of Crop Nutrition Science*, 18(2), pp. 254. DOI: https://doi.org/10.57647/ijes.2025.16945

Velázquez-Cruz, D., Espinosa-Castañeda, G., Díaz-Viera, M.A. and Leyte-Guerrero, F. 2017. New methodology for pore pressure prediction using well logs and divergent area. *SPE Latin America & Caribbean Petroleum Engineering Conference*, SPE-185557-MS, pp. 1–14. DOI: https://doi.org/10.2118/185557-MS

Weber, K.J. and Daukoru, E. 1975. Petroleum geology of the Niger Delta. Proceedings of the Ninth World Petroleum Congress, 2, pp. 209–221.

Xiao, H. and Suppe, J. 1992. Origin of rollover. *American Association of Petroleum Geologists Bulletin*, 76, pp. 509–529. DOI: https://doi.org/10.1306/bdff8858-1718-11d7-8645000102c1865d

Yilmaz, O. and Doherty, S.M. 2000. Seismic data analysis, processing, inversion, and interpretation of seismic data. *Society of Exploration Geophysicists, Tulsa, Investigations in Geophysics*, Vol. 10(2), p. 2027.

York, P., Prithard, D., Dodson, J.K., Dodson, T., Rosenberg, S., Gala, D. and Utama, B. 2009. Eliminating non-productive time associated with drilling trouble zone. *Offshore Technology Conference*, OTC 20220, Houston. DOI: https://doi.org/10.4043/20220-MS

Yu, H., Chen, G. and Gu, H. 2020. A machine learning methodology for multivariate pore-pressure prediction. *Computers & Geosciences*, 143, 104548. DOI: https://doi.org/10.1016/j.cageo.2020.104548

Zhang, G., Davoodi, S., Band, S.S., Ghorbani, H., Mosavi, A. and Moslehpour, M. 2022. A robust approach to pore pressure prediction applying petrophysical log data aided by machine learning techniques. *Energy Reports*, 8, pp. 2233–2247. DOI: https://doi.org/10.1016/j.egyr.2022.01.012

Zhang, J. 2011. Pore pressure prediction from well logs: Methods, modifications, and new approaches. *Earth Science Reviews*, 1, pp. 50–63. DOI: https://doi.org/10.1016/j.earscirev.2011.06.001

Zhao, J., Li, J. and Xu, Z. 2018. Advances in the origin of overpressures in sedimentary basins. *Petroleum Research*, 3, pp. 1–24. DOI: https://doi.org/10.1016/j.ptlrs.2018.03.007

Zijian, C., Jingen, D., Baohua, Y., Qiang, T. and Zhuo, C. 2015. The improvement methods of pore pressure prediction accuracy in Central Canyon in Qiongdongnan Basin. *4th International Conference on Environmental Energy and Biotechnology*, v. 85.